EurJIC European Journal of Inorganic Chemistry

ChemPubSoc Europe

FULL PAPER

DOI:10.1002/ejic.201500648

Luminescence and Relaxometric Properties of Heteropolymetallic Metallostar Complexes with Selectively Incorporated Lanthanide(III) Ions

Matthias Ceulemans,[a] Elke Debroye,[a] Luce Vander Elst,[b] Wim De Borggraeve,[a] and Tatjana N. Parac-Vogt*[a]

Keywords: Metallostars / Imaging agents / Luminescence / Gadolinium / Lanthanides

The synthesis and characterization of two diethylenetriaminepentaacetic acid (DTPA) based heteropolymetallic metallostar lanthanide complexes with the general formulas $(GdL^1)_3Ln$ and $(GdL^2)_3Ln$ are described. The synthesis uses a synthetic approach recently developed in our group for the selective complexation of gadolinium(III) and luminescent lanthanide ions with a ditopic ligand to form highly paramagnetic and luminescent metallostar complexes. The luminescence data and relaxometric studies suggest the potential applicability of the complexes as bimodal contrast agents for magnetic resonance and optical imaging. Owing to the higher excited state of L^1, better sensitization was observed for all $(GdL^1)_3Ln$ complexes than for $(GdL^2)_3Ln$. A large increase of the quantum yield from 1.5 to 9.8 % was observed for the $(GdL^1)_3Eu$ complex compared with $(GdL^2)_3Eu$, whereas the $(GdL^1)_3Tb$ complex exhibited a quantum yield (QY) of 30.9 % compared with 15.3 % for $(GdL^2)_3Tb$. A slight increase of the QY from 0.8 to 1.2 % was observed for the Dy(III) complex when switching from ligand L^2 to L^1. The nuclear magnetic relaxation dispersion (NMRD) measurements of the $(GdL^2)_3Ln$ complexes (Ln = Eu^{III}, Dy^{III}, Tb^{III}) showed respective longitudinal relaxivity (r_1) values of 24.27, 22.80 and 21.72 $s^{-1}mmol^{-1}$ per metallostar complex at 310 K and 20 MHz.

Introduction

The interest in contrast agents as efficient, responsive and tissue-specific markers has grown tremendously since the introduction of magnetic resonance imaging (MRI) as a diagnostic tool. Gadolinium(III) chelates have been used widely as MRI contrast agents.[1–5] Gadolinium(III) ions can efficiently induce relaxation of water molecules owing to their seven unpaired electrons, which produce a large magnetic moment (7.94 μ_B), and a symmetric $^8S_{7/2}$ ground state, which provides relatively long electron relaxation times.[1] Owing to the toxicity of free gadolinium(III) ions (LD_{50} = 0.2 mmol kg^{-1} in mice) and the relatively high doses of contrast agent needed (0.1–0.3 mmol per kg of body weight), the use of strong chelates is necessary.[6,7] Two of the most commonly used ligands for gadolinium(III) in modern molecular imaging techniques are the acyclic diethylenetriaminepentaacetic acid (DTPA; Magnevist®, Bayer Shering Pharma AG) and the cyclic 1,4,7,10-tetraazacyclododecane-1,4,7,10-tetraacetic acid (DOTA; Dotarem®, Guerbet).[2] The eightfold coordination of these ligands to gadolinium(III) ions ensures stable complexes with log K = 22.5 and 25.3 for DTPA and DOTA, respectively.[8–10] Furthermore, the eightfold coordination allows the binding of one water molecule to the metal centre, and the residence time of this water molecule (τ_m) is one of the four main parameters that govern the relaxivity r_1. The relaxivity describes the effectiveness of a contrast agent to induce relaxation and is defined by the increase of the longitudinal relaxation rate in s^{-1} measured in a 1 mM gadolinium(III) solution. In addition to the water residence time (τ_m), the other parameters that influence relaxivity are the relaxation behaviour of the electron spin of the gadolinium(III) ions ($\tau_{S1,2}$), the rotational correlation time of the complex in solution (τ_R) and the amount of water molecules directly bound to the gadolinium(III) ion (q).[9] Although the gadolinium(III) complexes currently used clinically have relaxivities of ca. 4–5 $s^{-1}mM^{-1}$, an increase of up to 100 $s^{-1}mM^{-1}$ could be achieved through the optimization of these different parameters according to the Solomon–Bloembergen–Morgan theory.[9,11] A frequently used approach towards increasing the relaxivity focuses on the increase of the rotational correlation time, for example, by conjugation of Gd^{III} chelates into linear polymers or dendrimers.[10,12–14] Another approach includes noncovalent interactions, such as the binding of chelates to human serum albumin, the most abundant protein in human plasma.[4,15,16] The formation of supramolecular structures such as micelles or liposomes from amphiphilic gadolinium(III) complexes[17–21] results in a high density of paramagnetic species and, simultaneously,

[a] Department of Chemistry, KU Leuven,
Celestijnenlaan 200F, 3001 Leuven, Belgium
E-mail: Tatjana.Vogt@chem.kuleuven.be
http://chem.kuleuven.be/lbc/
[b] Department of General, Organic and Biomedical Chemistry, University of Mons,
Place du Parc 23, 7000 Mons, Belgium

an increase in the rotational correlation time.[22] Although these approaches effectively increase the overall relaxivity of the contrast agent, the high theoretical maximum efficiency has unfortunately not yet been reached.

The MRI technique excels in its high spatial resolution and tissue penetration but suffers from a low sensitivity. Therefore, to remedy the low sensitivity of MRI, bimodal imaging has gained importance in recent years. Clinically, bimodal imaging combining positron emission tomography (PET) and MRI is already available.[23] This technique is able to provide high-quality three-dimensional images of soft tissue combined with the high sensitivity of PET imaging. On the other hand, optical imaging (OI) is also a very sensitive technique for which no ionizing radiation is necessary. The combination of both MRI and OI into one probe would allow images to reveal more details than those obtained from both techniques separately. The use of one contrast agent for both techniques would ensure the same distribution and reduce the stress imposed on the body by two different probes. The bimodal contrast agents for MRI/OI with organic fluorophores have several shortcomings including small Stokes shifts, short luminescence lifetimes and photobleaching. Therefore, increasing attention has been focused on luminescent lanthanide-based systems, which can emit light in the visible[24] and near-infrared regions.[25] However, tissue penetration is a very important factor when deciding which lanthanide to choose for in vivo probes. A good trade-off between the image resolution and penetration depth can be made in the wavelength region 665–900 nm.[26] Mixed-complex systems have been reported in which the generation of mixed micelles produces probes with high relaxivities and luminescence. Alternatively, the use of heteropolymetallic complexes has been investigated.[15,27–29] In addition to gadolinium(III) chelating moieties, these complexes must contain antenna links surrounding an emissive metal ion. However, the control of the site-selective incorporation of lanthanide ions within one ligand scaffold is a challenging task because of the similar complexation abilities across the lanthanide series.[30]

In a previous paper, we reported the successful synthesis of the heterotetrametallic complex $(Gd\mathbf{L^1})_3Eu$, in which two different lanthanide(III) ions were selectively incorporated into one ligand, $\mathbf{L^1}$. The resulting complex contained three Gd-DTPA moieties linked to a europium(III) chelate consisting of a *para*-substituted dipicolinic acid (DPA) and exhibited both high relaxivity, owing to the presence of three gadolinium(III) ions, and favourable europium(III) luminescence.[30] Encouraged by these results, in this work, we further extend this strategy toward the creation of potential bimodal contrast agents with selectively incorporated lanthanide ions. A series of $(Gd\mathbf{L^1})_3Ln$ complexes, in which Ln represents different luminescent lanthanide(III) ions, have been prepared. In addition, the new ligand $\mathbf{L^2}$, which contains an ethynyl linker between the two aromatic centres, has been synthesized with the aim to decrease the excited triplet state of the ligand to provide better energy transfer to ytterbium(III) ions.[31] By the same selective synthetic approach, a series of heterotetrametallic complexes based on this new ligand have been synthesized and characterized. The magnetic and luminescence properties of the complexes have been studied, and their potential as bimodal contrast agents for MRI and optical imaging has been evaluated.

Results and Discussion

Ligands and Complexes

The general ligand design is based on the attachment of a DTPA scaffold through an amide linkage to *para*-substituted dipicolinic acid (DPA), which has previously been demonstrated to form tris complexes with lanthanide(III) ions.[30] This approach allows the incorporation of different antennae between the two coordinating moieties to sensitize the luminescent lanthanide ions. The first method has been reported previously by our group and resulted in the synthesis of a Eu^{III} metallostar complex with the structure shown in Scheme 1.[30] A Suzuki–Miyaura coupling[32] was used to obtain a fully protected dipicolinate derivative, which allowed to selectively incorporate gadolinium(III) ions into the DTPA unit. The subsequent removal of the protecting groups and coordination to the luminescent europium(III) ions yielded the desired metallostar complex. In this work, the complexation to other luminescent lanthanide ions (Ln^{III} = Tb^{III}, Dy^{III}, Sm^{III}, Ho^{III}, Tm^{III} and Yb^{III}) has been performed by the same approach. This resulted in a range of metallostar complexes that all contain three gadolinium(III)–DTPA units but differ in the nature of the central lanthanide(III) ion bound to the dipicolinate units (Scheme 1).

The synthesis of the new ligand $\mathbf{L^2}$ makes use of Sonogashira cross-couplings and employs a slightly altered synthetic pathway than the one previously reported by Bünzli et al.[33] The first step is the protection of 4-iodobenzylamine with *t*-boc-anhydride (boc = butoxycarbonyl) to form **1** (Scheme 2). Compound **1** is subsequently coupled to trimethylsilylacetylene through a Sonogashira cross-coupling to form **2**, and subsequent deprotection of the trimethylsilyl group yields **3**. The NMR spectrum clearly shows the disappearance of the signals of the highly shielded trimethylsilyl protons at δ = 0.24 ppm and the appearance of a single peak of the ethynyl group at δ = 3.06 ppm. Compound **3** is able to undergo another Sonogashira cross-coupling with dimethyl 4-bromo-2,6-pyridinedicarboxylate under the same conditions to form **4**.

The *t*-Boc group is selectively deprotected by using trifluoroacetic acid in dichloromethane (50:50), as confirmed by the disappearance of the *tert*-butyl peaks at δ = 1.45 ppm and the persistence of the methyl peaks at δ = 4.06 ppm in the ^{1}H NMR spectrum. This approach results in a free amine (**5**), which can be coupled to the one free acid of the DTPA *tert*-butyl ester through amide synthesis to afford a fully protected ligand (**6**). Finally, the DTPA *tert*-butyl esters are selectively cleaved with a 6 M HCl solution to afford **7** (Scheme 3) The acidic groups of DTPA can then be further coordinated to gadolinium(III) ions. The complexation was performed with $GdCl_3{\cdot}6H_2O$ in pyridine, and the ab-

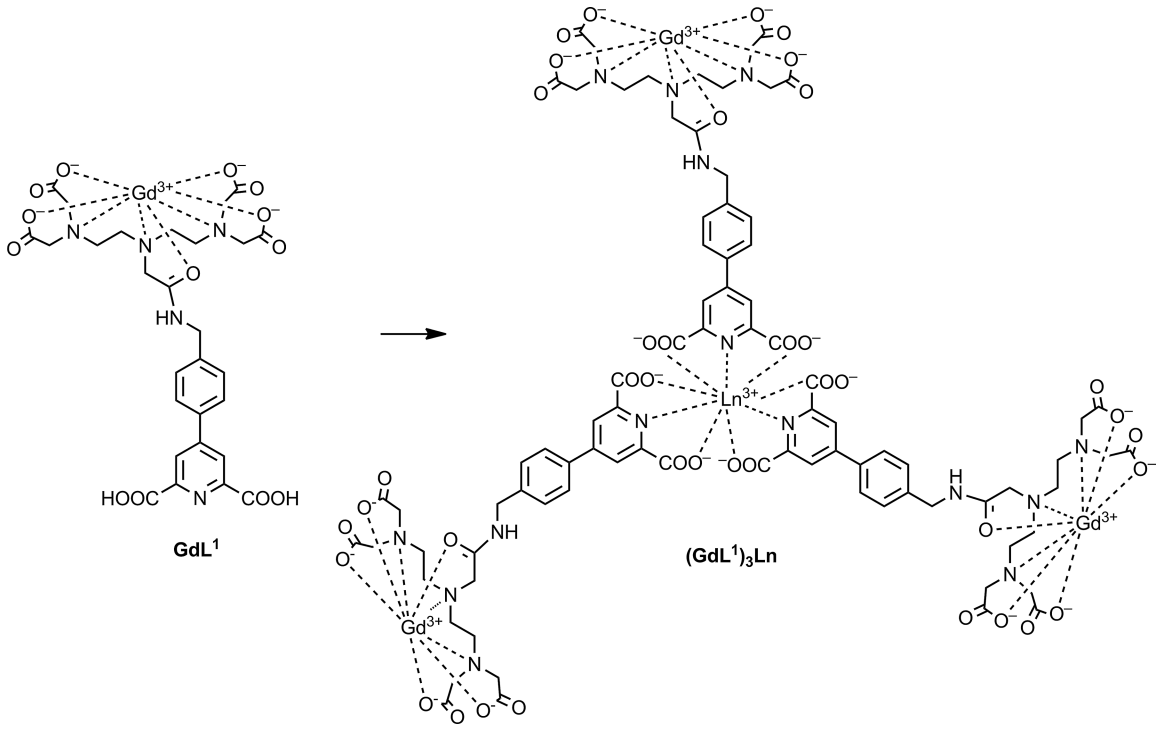

Scheme 1. Schematic representation of the complex Gd**L**^{1} and the heterotetrametallic metallostar (Gd**L**^{1})$_3$Ln (Ln = Eu^{III}[30] Dy^{III}, Tb^{III}, Ho^{III}, Nd^{III}, Sm^{III}, Tm^{III} and Yb^{III}).

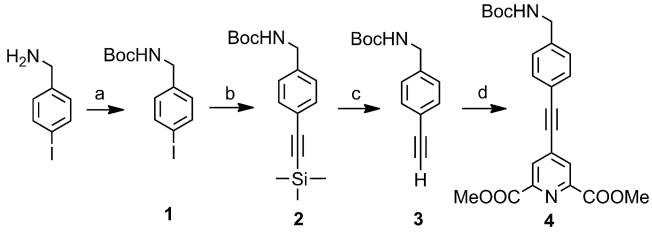

Scheme 2. Synthetic pathway to **L**^{2}: (a) boc-anhydride; (b) ethynyltrimethylsilane, $PdCl_2(PPh_3)_2$; (c) 1 M tetra-*n*-butylammonium fluoride (TBAF); (d) dimethyl 4-bromo-2,6-pyridinedicarboxylate, $PdCl_2(PPh_3)_2$.

sence of free lanthanide ions was verified by the addition of an arsenazo indicator solution.[34] The selective removal of the methyl ester protecting groups from the dipicolinate moiety was performed under alkaline conditions, and the final ligand was mixed with a luminescent lanthanide ($LnCl_3 \cdot xH_2O$) salt (Ln^{III} = Eu^{III}, Tb^{III}, Dy^{III}, Sm^{III}, Ho^{III}, Tm^{III}, Yb^{III}). By this approach, the desired metallostar tris complexes (Gd**L**^{2})$_3$Ln were generated, as is schematically shown in Scheme 4.

Photophysical Properties of the (GdL^{1})$_3$Ln and (GdL^{2})$_3$Ln Complexes

The absorption spectrum of the Gd**L**^{1} complex has a well-defined maximum at $\lambda \approx 282$ nm ($\varepsilon = 4250\ cm^{-1}\,M^{-1}$) caused by the $\pi \rightarrow \pi^*$ transition of DPA.[35] The excitation

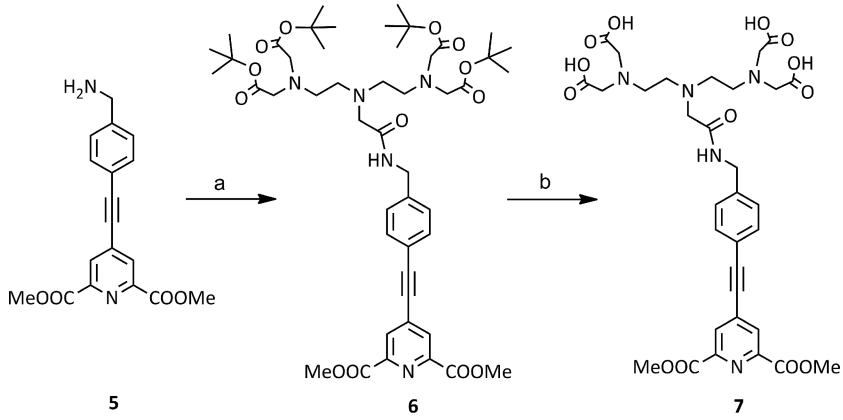

Scheme 3. Synthetic pathway to **L**^{2}: (a) DTPA *tert*-butyl ester, *O*-(benzotriazol-1-yl)-*N*,*N*,*N*′,*N*′-tetramethyluronium tetrafluoroborate (TBTU); (b) 6 M HCl.

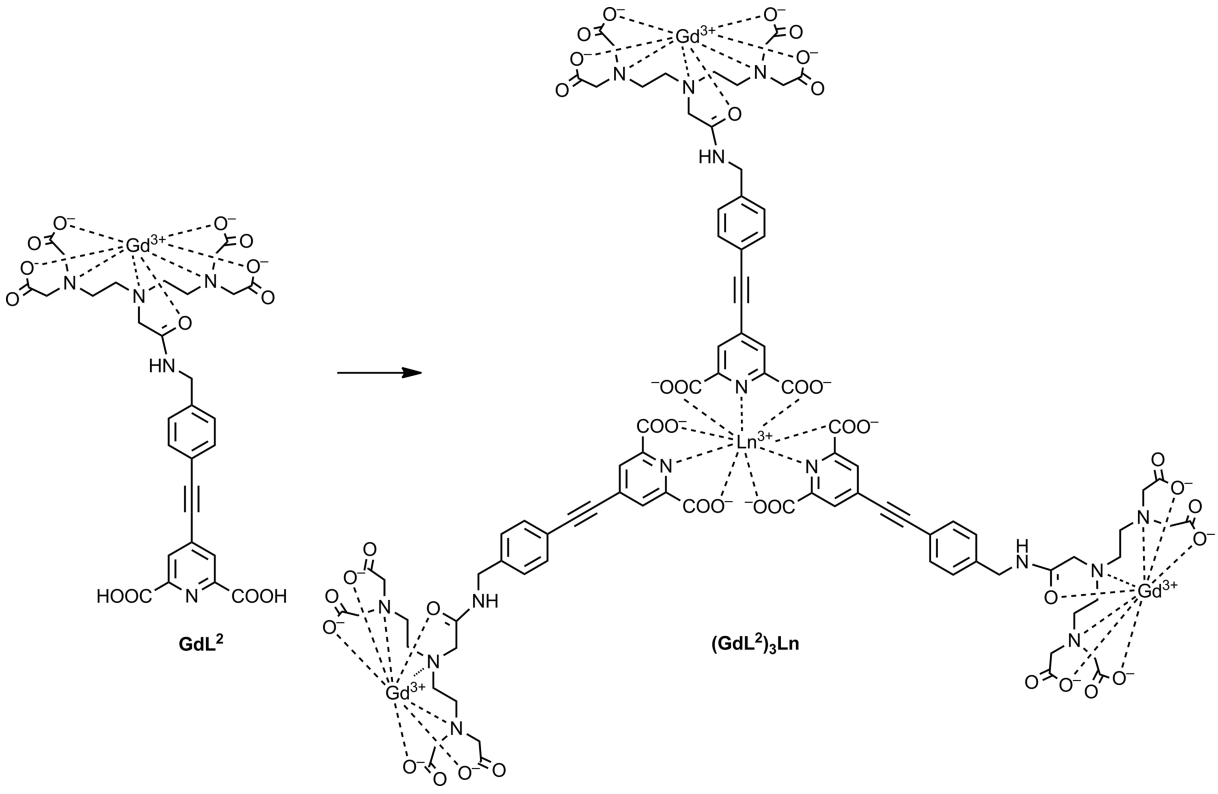

Scheme 4. Schematic representation of the complexes Gd**L²** and the heterotetrametallic metallostars (Gd**L²**)$_3$Ln (Ln = Eu^{III}, Dy^{III}, Tb^{III}, Nd^{III}, Sm^{III}, Tm^{III}, and Yb^{III}).

spectrum shows a broad band between λ = 250 and 300 nm with a maximum at 295 nm. The absorption spectra of Gd**L²** and the tris complex (Gd**L²**)$_3$Ln both show an absorption maximum at λ = 315 nm. The molar extinction coefficient of the free complex Gd**L²** at this maximum is ε_{315} = 6692 cm^{-1} M^{-1}, whereas the tris complex has ε_{315} = 11000 cm^{-1} M^{-1}. In the emission spectra of the (Gd**L¹**)$_3$Eu and (Gd**L²**)$_3$Eu metallostar complexes, the splitting of the $^5D_0 \rightarrow {}^7F_1$ transition into three bands suggests a slightly deformed D_3 symmetry around the central ion (Figure 1).[30,36] This is further supported by the ratio of the $^5D_0 \rightarrow {}^7F_2$ and $^5D_0 \rightarrow {}^7F_1$ transitions, which is ca. 5–6.

The luminescence decays of the metallostar complexes (Gd**L¹**)$_3$Eu and (Gd**L²**)$_3$Eu have been measured in water and D_2O, and the results are shown in Table 1. The shorter luminescence lifetime in water than that in D_2O is due to the presence of inner-sphere high-energy O–H vibrations and can be used to determine the number of coordinated water molecules. The best fit was observed by applying a biexponential decay, which suggests the presence of two different species in solution. The phenomenological equation for Ln^{III}–polyaminocarboxylate systems has been employed to determine the hydration number q with an accuracy of ±0.1; see Equation (1).[37,38]

$$q_{Eu(H_2O)} = 1.11(\Delta k_{obs} - 0.31 + 0.44q^{OH} + 0.99q^{NH} + 0.075q^{CONH}) \quad (1)$$

In Equation (1), Δk_{obs} represents the difference of the decay rate constants [$k_{H_2O} = 1/\tau_{H_2O}$ and $k_{D_2O} = 1/\tau_{D_2O}$] expressed in ms^{-1} for Eu^{III}. The q^X values represent the number of OH, NH or CONH groups bound directly to the lanthanide centre. For these calculations, only the contribution of the amide groups has been considered, that is, q^{CONH} = 1. The results indicate that an equilibrium has been set between the bis and tris complexes at the low concentrations used for luminescence measurements (2.0×10^{-5} M). These findings are consistent with those pre-

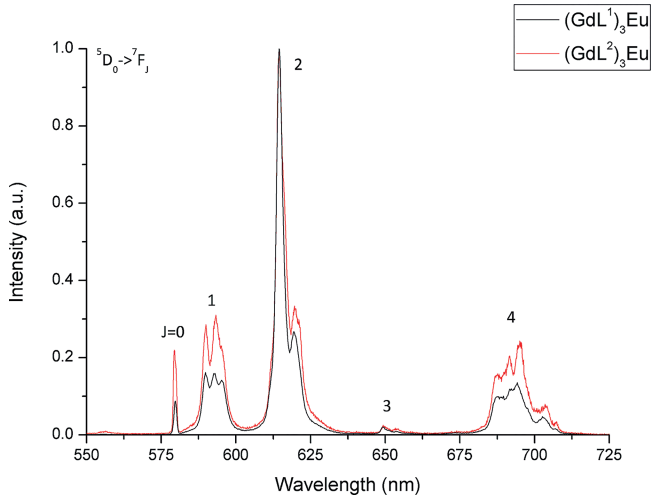

Figure 1. Corrected and normalized luminescence spectra of (Gd**L¹**)$_3$Eu (λ_{exc} = 293 nm, 298 K) and (Gd**L²**)$_3$Eu, (λ_{exc} = 315 nm, 298 K).

Table 1. Luminescence lifetimes of the different $(GdL)_3Ln$ complexes (Ln = Eu^{III}, Dy^{III}, Tb^{III}), average number of calculated water molecules in the first coordination sphere of the Ln ion (q) and the ratio of tris/bis complexes under the conditions of the measurements (2.0×10^{-5} M).

	H_2O	D_2O	q	Tris/bis ration
$(GdL^1)_3Eu$[a]	0.23 ms	1.12 ms	0.6	80:20
$(GdL^1)_3Dy$	9 μs	39 μs	1.2	85:15
$(GdL^1)_3Tb$	1.42 ms	2.42 ms	1.3	55:45
$(GdL^2)_3Eu$	0.20 ms	1.11 ms	0.2	96:4
$(GdL^2)_3Dy$	9 μs	14 μs	0.3	90:10
$(GdL^2)_3Tb$	2.20 ms	2.40 ms	0.8	73:27

[a] From ref.[30]

viously reported for $(DPA)_3Eu$ complexes, for which a significant amount of the bis complex was detected in micromolar concentrations.[39] As no water is present in the first coordination sphere of the central ion in the tris complex, whereas the bis complex should have three water molecules bound, this allows the determination of the ratio between the tris and bis complexes. An increase of the ratio of tris to bis complex from 80:20 for $(GdL^1)_3Eu$ to 95:5 for $(GdL^2)_3Eu$ is seen upon the introduction of an ethynyl linker to the ligand structure. The luminescence quantum yields Q_L^{LN} were determined upon ligand excitation by a comparative method with a solution of rhodamine 101 in ethanol (Q = 100%) as the standard. The quantum yield was determined according to Equation (2):

$$Q_L^{Ln} = Q_S \times \frac{I_X}{I_S} \times \frac{A_S(\lambda_{exc})}{A_X(\lambda_{exc})} \times \frac{\eta_X^2}{\eta_S^2} \quad (2)$$

In this equation, s and x refer to the standard and the unknown sample, respectively, I represents the corrected total integrated emission intensity, A is the absorbance at the excitation wavelength, and η is the refractive index of the solution (η_{water} = 1.33 and $\eta_{ethanol}$ = 1.36). The quantum yields are summarized in Table 2. Owing to the lower π–π* energy level of Gd**L²**, the quantum yield of the complex drops from 9.8% for $(GdL^1)_3Eu$ to 1.5% for $(GdL^2)_3Eu$; therefore, **L²** is a less efficient sensitizer of europium emission. The direct excitation of the lanthanide ions is possible but is very inefficient because the f–f transitions are Laporte forbidden. However, the intrinsic quantum yields Q_{Ln}^{LN} (Ln^{III} = Eu^{III}, Tb^{III}) can be estimated from Equations (3) and (4) for the ratio between the observed (τ_{obs}) and radiative (τ_{rad}) lifetimes.

Table 2. Calculated quantum yields of $(GdL^1)_3Ln$ (λ_{exc} = 293 nm, 298 K) and $(GdL^2)_3Ln$ (λ_{exc} = 315 nm, 298 K).

Ln	H_2O	D_2O
Eu	9.8%	1.5%
Dy	1.2%	0.8%
Tb	30.9%	15.3%

The Einstein coefficient $A_{MD,0}$ equals 14.65 s^{-1}, n is the refractive index set to n_{H_2O} = 1.34, which is equal to that of the neat solvent, and (I_{tot}/I_{MD}) represents the ratio of the total integrated intensity of the transitions to the transition

$$\frac{1}{\tau_{rad}} = A_{MD,0} \times n^3 \times \left(\frac{I_{tot}}{I_{MD}}\right) \quad (3)$$

$$Q_{Ln}^{Ln} = \frac{\tau_{obs}}{\tau_{rad}} \quad (4)$$

of the magnetic dipole (MD). The intrinsic quantum yield values Q_{Eu}^{Eu} for both Gd**L¹** and Gd**L²** are in the range 22–24%. Finally, we can acquire the ratio between the quantum yield under ligand excitation and the intrinsic quantum yield to obtain the sensitization efficiency (η_{sens}) of the ligand; see Equation (5).

$$\eta_{sens} = \frac{Q_L^{Eu}}{Q_{Eu}^{Eu}} \quad (5)$$

This results in sensitization efficiencies of 47% for $(GdL^1)_3Eu$ and only 6.3% for $(GdL^2)_3Eu$. These values are lower than those for the parent $(DPA)_3Eu$ complex, which has Q_{Eu} = 24% and η_{sens} = 61%.[35]

Dysprosium(III) complexes with Gd**L¹** and Gd**L²** showed yellow emission owing to $^4F_{9/2} \rightarrow {}^6H_J$ (J = 15/2, 13/2 and 11/2) transitions. However, owing to the poor sensitization of the ligands towards dysprosium(III) ions, some ligand emission is also observed (Figure 2). $(GdL^1)_3Dy$ clearly shows the three transitions of the Dy(III) centre with some ligand emission, whereas the $(GdL^2)_3Dy$ emission spectrum is dominated by ligand emission. The $^4F_{9/2} \rightarrow {}^6H_{15/2}$ transition, which is typically observed at λ = 485 nm, has completely disappeared under the ligand emission tail. However, the $^4F_{9/2} \rightarrow {}^6H_{13/2}$ transition, which is located at $\lambda \approx$ 575 nm is clearly visible together with the weak $^4F_{9/2} \rightarrow {}^6H_{11/2}$ transition at λ = 665 nm. The quantum yields for the dysprosium(III) samples have been measured with a solution of rhodamine 101 in ethanol (Q = 100%) as a standard. From Equation (2), low values of 1.2% for $(GdL^1)_3Dy$ and 0.8% for $(GdL^2)_3Dy$ were obtained

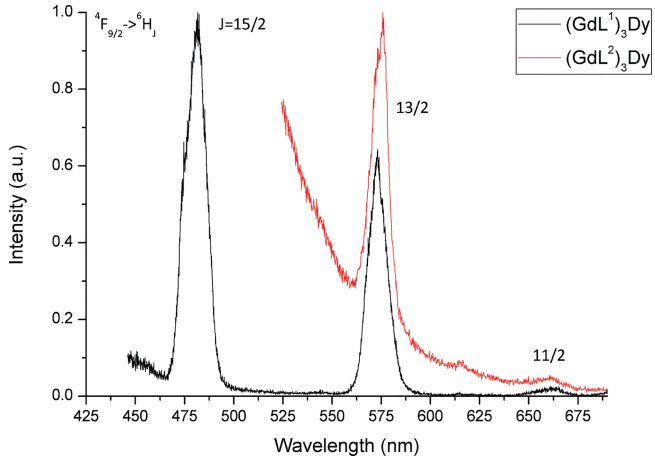

Figure 2. Corrected and normalized luminescence spectra of $(GdL^1)_3Dy$ (λ_{exc} = 293 nm, 298 K) and $(GdL^2)_3Dy$ (λ_{exc} = 315 nm, 298 K).

(Table 2). The poor efficiency of the ligands to sensitize dysprosium(III) ions could be observed in the luminescence spectra. The amounts of water molecules were calculated by using the phenomenological Equation (6).[19,40,41] The values of 1.2 and 0.3 obtained for $(GdL^1)_3Dy$ and $(GdL^2)_3Dy$ result in ratios of the tris complex to bis complex of 85:15 and 90:10, respectively.

$$q_{Dy(H_2O)} = 21.1 \times \Delta k_{obs} - 0.60 \quad (6)$$

The characteristic green emission was observed for the terbium(III) complexes GdL^1 and GdL^2 with the ligand excited at λ = 295 and 315 nm respectively, owing to the Tb^{III} $^5D_4 \rightarrow {}^7F_J$ (J = 6–0) transitions (Figure 3). The quantum yields for the terbium(III) complexes are relatively high and were measured to be 30% for $(GdL^1)_3Tb$ and 15% for $(GdL^2)_3Tb$ by the comparative rhodamine 101 method. The amount of water molecules bound to the luminescent centre can also be determined from lifetime measurements in H_2O and D_2O by using Equation (7),[37,42] and the results are shown in (Table 2).

$$q_{Tb(H_2O)} = 5 \times (\Delta k_{obs} - 0.06) \quad (7)$$

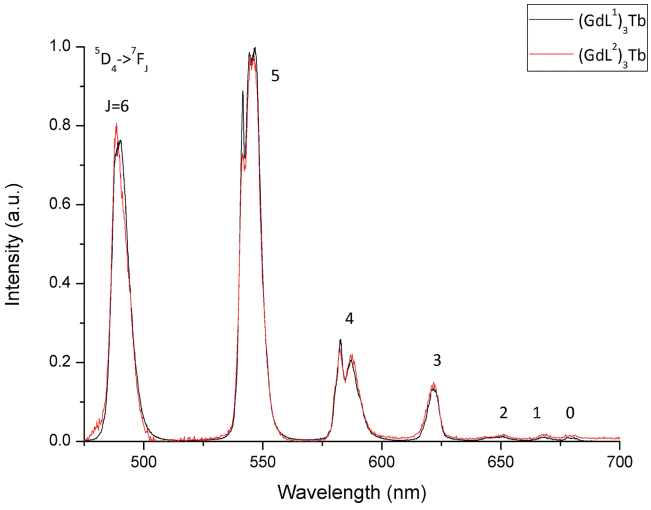

Figure 3. Corrected and normalized luminescence spectra of $(GdL^1)_3Tb$ (λ_{exc} = 293 nm, 298 K) and $(GdL^2)_3Tb$ (λ_{exc} = 315 nm, 298 K).

The overall ratios of the tris to bis complexes for $(GdL^1)_3Tb$ and $(GdL^2)_3Tb$ are 55:45 and 73:27, respectively. These ratios are lower than those for the other lanthanides, but very high quantum yields can still be obtained, apparently because the energy from the excited state of terbium(III) is poorly quenched by water.

The tris complexes of all other luminescent lanthanide ions such as neodymium(III), holmium(III), samarium(III) or thulium(III) unfortunately only give rise to ligand emission, and no distinct peaks for lanthanide emission could be observed. The low energy of the π–π* state apparently makes both L^1 and L^2 poor sensitizers for these lanthanides. However, for the ytterbium(III) complex $(GdL^2)_3Yb$, solid-state emission at λ = 980 nm corresponding to the $^2F_{5/2} \rightarrow {}^2F_{7/2}$ transition could be observed (Figure 4), whereas emission was absent for $(GdL^1)_3Yb$. Luminescence in the IR region was not seen for aqueous solutions of either $(GdL^1)_3Yb$ or $(GdL^2)_3Yb$, most likely because of the quenching of the radiative emission by water.

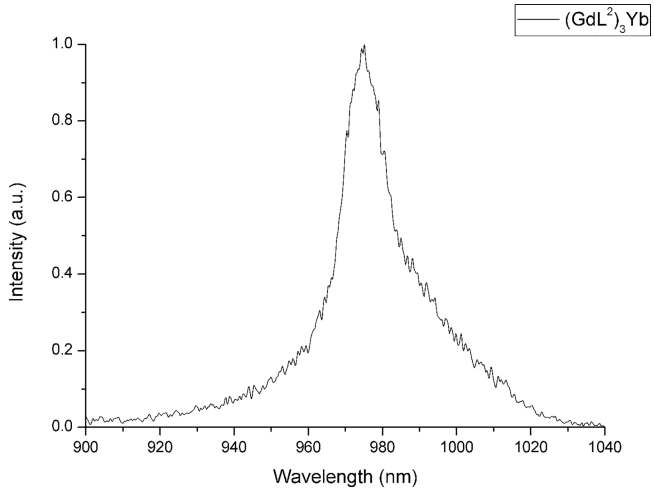

Figure 4. Corrected and normalized solid-state luminescence spectra of $(GdL^2)_3Yb$, λ_{exc} = 315 nm, 298 K.

Relaxometric Studies

The efficiency of a 1 mM solution of a gadolinium(III) agent to shorten the longitudinal relaxation time (T_1) can be derived from proton nuclear magnetic relaxation dispersion (NMRD) profiles by measuring the water proton relaxivity (r_1) as a function of the magnetic field strength. The relaxation rate is enhanced by the dipolar interaction between the water molecules and the paramagnetic gadolinium(III) centre. In addition to inner-sphere contributions,[11,42] which result from the water molecules directly bound to the paramagnetic centre and exchanging with the bulk, outer-sphere[43] interactions of water have to be taken into account; in some cases, second-sphere interactions[44,45] can also have significant effects. Several parameters are defined for the inner-sphere water molecules. Although water molecules directly bound to the luminescent centre have a negative effect on the luminescence, a high relaxivity can be obtained with a higher amount of water molecules directly bound to the paramagnetic centre (q). Other parameters are the distance between the gadolinium(III) centre and the water molecules (r), the water residence time (τ_M), the rotational correlation time of the paramagnetic centre (τ_R), the electronic relaxation time of gadolinium(III) at zero field (τ_{S0}) and the correlation time that modulates the electronic relaxation (τ_v).

The ^1H NMRD profiles of GdL^1 and $(GdL^1)_3Eu$ have been reported in our recent publication.[30] The profile of $(GdL^1)_3Eu$ displays a characteristic hump between 20 and 100 MHz, which is assigned to the formation of a supramolecular structure. At 20 MHz and 310 K, the relaxivity is enhanced to 8.3 s^{-1} mM^{-1} for GdL^1 and to 9.6 s^{-1} mM^{-1}

Table 3. Parameters obtained by fitting the ^{1}H NMRD data in water at pH 7.4 and 310 K. Fixed values: q = 1, r = 0.31 nm, d = 0.36 nm and $D = 3.0 \times 10^{-9}$ m^2 s^{-1}.

	Gd-DTPA[a]	Gd**L**^{2}[b]	(Gd**L**^{2})$_3$Eu[b]	(Gd**L**^{2})$_3$Dy[b]	(Gd**L**^{2})$_3$Tb[b]
τ_R [ps]	54 ± 1	809 ± 48	1000 ± 3	818 ± 35	916 ± 41
τ_{S0} [ps]	87 ± 3	83 ± 1	64 ± 1	70 ± 1	66 ± 1
τ_V [ps]	25 ± 3	20 ± 1	21 ± 1	18 ± 1	17 ± 1

[a] From ref.[46] [b] τ_M was fixed to 1500 ns.

for (Gd**L**^{1})$_3$Eu compared with 3.8 s^{-1} mM^{-1} for Gd-DTPA, as could be expected given the higher molecular weight of the synthesized chelates. With the presence of three gadolinium ions per metallostar compound considered, a longitudinal relaxation rate of 28.8 s^{-1} mM^{-1} per (Gd**L**^{1})$_3$Eu molecule is obtained at 20 MHz and 310 K.

In this work, the relaxometric properties of metallostars based on the **L**^{2} ligand have been examined (Table 3). Similarly to that of (Gd**L**^{1})$_3$Eu, each of the proton NMRD profiles of the (Gd**L**^{2})$_3$Ln metallostars (measured in water at pH 7.4 and 310 K) show a hump between 20 and 100 MHz, characteristic of supramolecular structures in solution (Figure 5). The similarity of the NMRD profile of Gd**L**^{2} to those of the metallostar complexes suggests a self-aggregation of the monomer to form dimeric, trimeric or multimeric species.

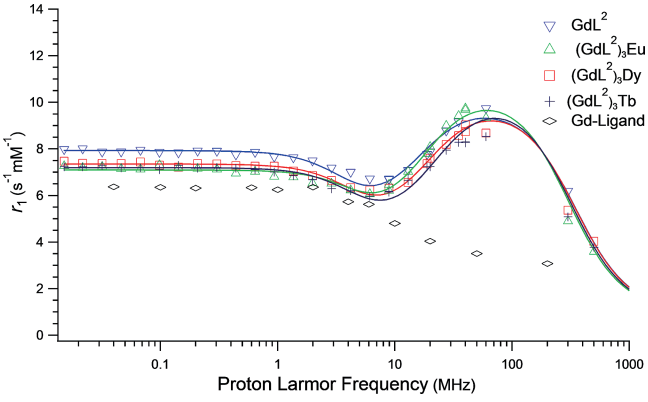

Figure 5. NMRD profiles of Gd**L**^{2} and (Gd**L**^{2})$_3$Ln (Ln = Eu, Dy and Tb) compared with that of Gd-DTPA in water at 310 K.

The NMRD data shown in Figure 5 were fitted to the Solomon–Bloembergen–Morgan equation, which indicated significant increases of τ_R compared with that of Gd-DTPA, as expected. However, owing to the possible equilibria between the tris and bis complexes, the precise τ_R values are difficult to determine. It should be noted that the equilibria between the tris and bis complexes observed in the luminescence measurements might be absent or present to a lesser extent owing to the higher concentrations used in the NMRD measurements. Also, from the stability constants of the Ln-DTPA and Ln(DPA)$_3$ complexes, it is plausible that the redistribution of Gd^{III} and Eu^{III} ions between both the ligands may occur. However, this is unlikely as the emission spectra of (Gd**L**^{1})$_3$Eu and (Gd**L**^{2})$_3$Eu do not show the splitting of the $^5D_0 \rightarrow {}^7F_1$ transition, which would be expected to occur if the Eu^{3+} ions were complexed in the DTPA-part. The relaxivities measured at 20 MHz at temperatures of 25–45 °C increased by less than 13%, which indicates a slow water exchange. Thus, during the fitting procedure, τ_M was fixed to 1500 ns for all of the metallostars as well as for the Gd**L**^{2} complex. At 20 MHz and 310 K, the relaxivity of the complexes (Gd**L**^{2})$_3$Ln with Ln = Eu^{III}, Dy^{III} and Tb^{III} were determined to be very similar (8.09, 7.60 and 7.24 s^{-1} mmol^{-1} respectively). Assuming the presence of three Gd-DTPA moieties, the expected r_1 relaxivities of the molecules would be 24.27, 22.8 and 21.72 s^{-1} mmol^{-1} per metallostar complex; these values are slightly lower than the value of 28.8 s^{-1} mM^{-1} observed for the (Gd**L**^{1})$_3$Eu metallostar.[30]

Conclusions

In this work, the selective incorporation of several lanthanides into two ditopic ligands has been accomplished, and the resultant metallostar complexes exhibited favourable luminescence and relaxometric properties for potential use as bimodal MRI/OI agents. The incorporation of Eu^{III}, Dy^{III} and Tb^{III} ions into the complexes resulted in emission in the visible region upon excitation into the ligand levels. Quantum yields of up to 10% for (Gd**L**^{1})$_3$Eu were achieved with a sensitization efficiency (η_{sens}) of 47%. The introduction of a ligand with an ethynyl group (Gd**L**^{2}) lowered the energy of the π–π* excited state, which resulted in a decrease of the quantum yield of the (Gd**L**^{2})$_3$Eu complex to 1.5% and a decrease of the sensitization efficiency to only 6.3%. The same effect has been observed for the dysprosium(III) and terbium(III) complexes. At the concentrations used in the luminescence measurements, the tris complexes partially converted into bis complexes; however, the presence of an extra linker between the aromatic rings in Gd**L**^{2} allowed for a larger tris to bis complex ratio compared with that for Gd**L**^{1}. The lower energy resulting from this linker also lowered the π–π* excited state of Gd**L**^{2} and allowed it to sensitize ytterbium(III) ions in the solid state. The NMRD profiles of (Gd**L**^{2})$_3$Ln complexes displayed characteristic humps between 20 and 100 MHz owing to the formation of supramolecular structures with enhanced longitudinal relaxivities of up to 25 s^{-1} mM^{-1} per metallostar assembly at 20 MHz and 310 K.

Experimental Section

Materials, Reagents and Solvents: Materials, reagents and solvents were obtained from Sigma–Aldrich (Bornem, Belgium), Acros Organics (Geel, Belgium), ChemLab (Zedelgem, Belgium), ABCR (Karlsruhe, Germany), Iris Biotech GmbH (Marktredwitz, Ger-

many) and BDH Prolabo (Leuven, Belgium) and were used without further purification. The gadolinium(III) salt was obtained from Alfa Aesar (Ward Hill, USA), and europium(III) chloride hexahydrate and lanthanum(III) chloride heptahydrate were obtained from Acros Organics (Geel, Belgium).

General Synthesis of $(GdL^1)_3Ln$: All complexes were synthesized by applying the previously reported procedure[30] and by replacing $EuCl_3$ with the appropriate $LnCl_3{\cdot}xH_2O$ salt. The complexes were characterized by total reflection X-ray fluorescence (TXRF), IR and optical spectroscopy. The Gd/Ln ratios obtained by TXRF spectroscopy were 2.6 (Gd/Tb), 2.8 (Gd/Dy), 3.0 (Gd/Ho), 3.0 (Gd/Sm), 3.1 (Gd/Nd) and 3.0 (Gd/Yb).

Compound 1: 4-Iodobenzylamine (1 equiv., 0.680 g, 2.92 mmol) and triethylamine (1.5 equiv., 4.38 mmol, 0.443 g) were dissolved in tetrahydrofuran (THF; 20 mL). The solution was cooled in an ice bath, and boc-anhydride (1.5 equiv., 4.38 mmol, 0.955 g) was added slowly. The mixture was stirred overnight at room temperature, and the solvent was evaporated. Water was added (20 mL), and the product was extracted with EtOAc (3 × 20 mL). The combined organic layer was washed with brine and dried with $MgSO_4$. The solvent was evaporated to yield the desired product (0.966 g, 99%). ESI-MS (MeOH): *m*/*z* = 356.6 $[M + Na]^+$. ^1H NMR (300 MHz, $CDCl_3$, 25 °C): δ = 1.45 (s, 9 H, *t*Bu), 4.23 (d, $^3J_{H,H}$ = 5.6 Hz, 2 H, NHCH_2C), 4.87 (br., 1 H, N*H*CH_2C), 7.01 (d, $^3J_{H,H}$ = 8.4 Hz, 2 H, ICCH$_2$CH_2C), 7.65 (d, $^3J_{H,H}$ = 8.4 Hz, 2 H, ICCH_2CH$_2$C) ppm. ^{13}C NMR (75 MHz, $CDCl_3$, 25 °C): δ = 28.38, 44.10, 79.71, 92.59, 129.36, 137.62, 138.73, 155.83 ppm.

Compound 2: The synthesis involved a similar procedure to that previously reported by Bünzli and co-workers[31] with (4-aminobenzyl)acetylene and dimethyl 4-bromopyridine-2,6-carboxylate. Compound **1** (1 equiv., 0.966 g, 2.90 mmol), bis(triphenylphosphine)palladium(II) chloride (5 mol-%, 0.101 mg, 0.145 mmol), copper(II) iodide (10 mol-%, 0.055 g, 0.290 mmol), and triethylamine (2 equiv., 0.587 g, 5.80 mmol) were suspended in dry THF (10 mL), and the mixture was stirred for 15 min under an inert atmosphere. Afterwards, (trimethylsilyl)acetylene (1.2 equiv., 0.118 g, 1.2 mmol) was added, and the mixture was stirred overnight. Diethyl ether (50 mL) was added, and the mixture was filtered through Celite. Purification over silica with chloroform yielded the desired product (0.704 g, 80%). ESI-MS (MeOH): *m*/*z* = 326.5 $[M + Na]^+$. ^1H NMR (300 MHz, $CDCl_3$, 25 °C): δ = 0.24 (s, 9 H, SiCH_3), 1.45 (s, 9 H, *t*Bu), 4.29 (d, $^3J_{H,H}$ = 5.6 Hz, 2 H, NHCH_2C), 4.85 (br., 1 H, N*H*CH_2C), 7.20 (d, $^3J_{H,H}$ = 7.6 Hz, 2 H, CCH$_2$CH_2C), 7.42 (d, $^3J_{H,H}$ = 7.6 Hz, 2 H, CCH_2CH$_2$C) ppm. ^{13}C NMR (75 MHz, $CDCl_3$, 25 °C): δ = 0.37, 28.34, 44.46, 79.68, 94.18, 104.86, 122.11, 127.23, 132.20, 139.43, 155.88 ppm.

Compound 3: Compound **2** (1 equiv., 0.671 g, 2.21 mmol) was dissolved in THF (20 mL), and the solution was cooled to 0 °C. TBAF (1 M, 4.02 mL, 4.42 mmol) was added, and the mixture was stirred at 0 °C for 1 h. After the reaction, a water/dichloromethane (water/DCM) mixture (50 mL) was added. The organic layer was collected and dried, and the solvents were evaporated. The crude product was purified with silica (eluent DCM) to afford the product (0.382 g, 75%). ESI-MS (MeOH): *m*/*z* = 354.6 $[M + Na]^+$. ^1H NMR (300 MHz, $CDCl_3$, 25 °C): δ = 1.45 (s, 9 H, *t*Bu), 3.1 (s, 1 H, CC*H*), 4.30 (d, $^3J_{H,H}$ = 5.9 Hz, 2 H, NHCH_2C), 4.90 (br., 1 H, N*H*CH_2C), 7.23 (d, $^3J_{H,H}$ = 8.3 Hz, 2 H, CCH$_2$CH_2C), 7.44 (d, $^3J_{H,H}$ = 8.3 Hz, 2 H, CCH_2CH$_2$C) ppm. ^{13}C NMR (75 MHz, $CDCl_3$, 25 °C): δ = 28.38, 44.37, 79.70, 83.43, 121.02, 127.1, 127.29, 132.34, 139.84, 155.87 ppm.

Compound 4: Dimethyl 4-bromopyridine-2,6-carboxylate (1 equiv., 0.411 g, 1.50 mmol), CuI (10 mol-%, 28.6 mg, 0.15 mmol) and bis(triphenylphosphine)palladium(II) chloride (5 mol-%, 52.7 mg, 0.075 mmol) were added to dry THF (10 mL). Triethylamine (2 equiv. 0.304 g, 3.00 mmol) was added, and the mixture was stirred for 15 min. Compound **3** (1.1 equiv., 0.382 g, 1.65 mmol) was added, and the mixture was stirred for 4 h at 40 °C. The THF was evaporated, CH_2Cl_2 was added, and the suspension was washed with water. The crude product was dissolved in methanol, and the solution was stirred for 30 min. The precipitate was collected by filtration and dried to afford the desired product (0.535 g, 84%). ESI-MS (MeOH): *m*/*z* = 447.7 $[M + Na]^+$. ^1H NMR (300 MHz, $CDCl_3$, 25 °C): δ = 1.47 (s, 9 H, *t*Bu), 4.04 (s, 6 H, O*Me*), 4.36 (d, $^3J_{H,H}$ = 6.1 Hz, 2 H, NHCH_2C), 4.92 (br., 1 H, N*H*CH_2C), 7.31 (d, $^3J_{H,H}$ = 8.1 Hz, 2 H, CCH$_2$CH_2C), 7.50 (d, $^3J_{H,H}$ = 8.1 Hz, 2 H, CCH_2CH$_2$C), 8.36 (s, 2 H, CCH_2CC) ppm. ^{13}C NMR (75 MHz, $CDCl_3$, 25 °C): δ = 28.39, 44.36, 53.33, 79.83, 85.41, 96.79, 120.24, 127.54, 129.65, 132.36, 132.73, 141.15, 148.44, 155.88, 164.75 ppm.

Compound 5: Compound **4** (1 equiv. 0.212 g, 0.5 mmol) was dissolved in a 50:50 dichloromethane/trifluoroacetic acid (DCM/TFA) mixture (10 mL), and the solution was stirred for 12 h at room temperature. The solvents were evaporated, DCM/MeOH (6:4, 10 mL) was added, and the solvents were evaporated again. The crude product was dissolved in DCM, washed with a saturated aqueous $NaHCO_3$ solution and brine and then dried with $MgSO_4$, yield 93%. ESI-MS (MeOH): *m*/*z* = 347.7 $[M + Na]^+$. ^1H NMR (300 MHz, [D$_5$]pyridine, 25 °C): δ = 3.91 (s, 6 H, O*Me*), 4.68 (s, 2 H, NHCH_2C), 4.92 (br., 1 H, N*H*CH_2C), 7.72 (d, $^3J_{H,H}$ = 7.9 Hz, 2 H, CCH$_2$CH_2C), 7.83 (d, $^3J_{H,H}$ = 7.9 Hz, 2 H, CCH_2CH$_2$C), 8.37 (s, 2 H, CCH_2CC) ppm. ^{13}C NMR (75 MHz, $CDCl_3$, 25 °C): δ = 53.33, 85.24, 97.02, 119.75, 127.38, 129.63, 132.01, 132.14, 132.32, 134.59, 148.40, 164.75 ppm.

Compound 6: Compound **5** (1.1 equiv., 0.28 mmol, 0.90 g) was dissolved in dry *N*,*N*-dimethylformamide (DMF, 10 mL), and *N*,*N*-diisopropylethylamine (1.5 equiv., 0.38 mmol, 66 μL) was added to the solution. The mixture was stirred for 15 min at room temperature under an inert atmosphere. At the same time, the DTPA *tert*-butyl ester (1 equiv., 0.25 mmol, 0.156 g), *O*-(benzotriazol-1-yl)-*N*,*N*,*N*′,*N*′-tetramethyluronium tetrafluoroborate (TBTU; 1.5 equiv., 0.38 mmol, 0.121 g) and *N*,*N*-diisopropylethylamine (1 equiv.; 0.25 mmol; 44 μL) were dissolved in dry DMF (10 mL) in a three-neck flask, and the solution was stirred for 15 min at room temperature under an argon atmosphere. The solution from flask 1 was added dropwise over a period of 10 min to the three-neck flask, and the mixture was stirred at room temperature under an argon atmosphere for 24 h. After the evaporation of the solvent, the residue was redissolved in DCM. The suspension was washed with a saturated aqueous $NaHCO_3$ solution and with brine. The organic phase was dried with magnesium sulfate and evaporated under reduced pressure. The obtained product was further purified through silica column chromatography (eluent: $CHCl_3$/5% MeOH/0.66% NH_3), and the collected fractions were evaporated and dried under vacuum at 50 °C to yield a yellow oil (0.196 mmol, 0.181 g, 70%). ESI-MS (MeOH): *m*/*z* = 947.4 $[M + Na]^+$. ^1H NMR (300 MHz, $CDCl_3$): δ = 1.44 (s, 36 H, *t*Bu), 2.64 (t, 4 H, NCH_2CH$_2$N), 2.78 (t, 4 H, NCH$_2$CH_2N), 3.24 [s, 2 H, NCH_2C(O)-NH], 3.33 [s, 8 H, NCH_2C(O)O], 4.04 (s, 6 H, O*Me*), 4.51 (d, $^3J_{H,H}$ = 6.2 Hz, 2 H, NHCH_2C), 7.38 (d, $^3J_{H,H}$ = 8.2 Hz, 2 H, CCH$_2$CH_2C), 7.53 (d, $^3J_{H,H}$ = 8.2 Hz, 2 H, CCH_2CH$_2$C), 8.35 (s, 2 H, CCH_2CC), 8.88 (br., 1 H, N*H*CH_2C) ppm. ^{13}C NMR (75 MHz, $CDCl_3$, 25 °C): δ = 28.16, 28.42, 38.61, 42.67, 52.10, 53.32, 53.76, 55.69, 81.09, 85.10, 97.31, 119.65, 128.13, 129.59, 132.13, 134.67, 142.06, 148.43, 164.77, 170.51 ppm.

Compound 7: The protected ligand precursor **6** (1 equiv., 0.19 mmol, 0.175 g) was dissolved in a 6 M HCl solution, and the mixture was stirred for 1 h at room temperature under an argon atmosphere. The solvent was evaporated, water was added, and the solution was evaporated again (2×). The product was redissolved in water, and the pH was adjusted from ca. 2 to 7 with pyridine. The solvents were evaporated and dried under vacuum at 50 °C to afford the product (0.176 mmol, 93%). ^{1}H NMR (300 MHz, [D$_5$]-pyridine, 25 °C): δ = 2.64 (t, 4 H, NCH_2CH$_2$N), 2.78 (t, 4 H, NCH$_2$CH_2N), 3.24 [s, 2 H, NCH_2C(O)NH], 3.91 (s, 6 H, O*Me*), 4.15 [s, 8 H, NCH_2C(O)O], 4.80 (d, $^3J_{H,H}$ = 6.4 Hz, 2 H, NHCH_2C), 7.57 (d, $^3J_{H,H}$ = 8.3 Hz, 2 H, CCH$_2$CH_2C), 7.62 (d, $^3J_{H,H}$ = 8.3 Hz, 2 H, CCH_2CH$_2$C), 8.35 (s, 2 H, CCH_2CC) ppm.

Synthesis of Methyl-Protected GdL^2: The methyl-protected ligand **7** (1 equiv., 0.23 mmol, 160 mg) was dissolved in pyridine (5 mL), and the hydrated GdCl$_3$ salt (1.05 equiv., 0.24 mmol) in water (0.3 mL) was added to the solution. This mixture was stirred for 3 h at 70 °C. The solvent was removed under reduced pressure, and ethanol was added. The suspension was heated under reflux for 1 h and then filtered through a P4 glass filter. The absence of free lanthanide ions was checked by using an arsenazo indicator.

Synthesis of GdL^2: The methyl-protected Gd**L^2** complex (1 equiv., 0.106 g, 0.12 mmol) was dissolved in water (5 mL), and K_2CO_3 (2.5 equiv., 0.31 mmol, 43 mg) was added to the solution. The mixture was stirred overnight at room temperature. After the completion of the reaction, a pH of ca. 9 was measured. The solvent was evaporated, water was added, and the solution was stirred for 30 min, after which the pH changed to ca. 8. The solvent was removed under reduced pressure, and orange flakes were obtained (0.11 mmol, 95%).

General Synthesis of (GdL^2)$_3$Ln: The deprotected Gd**L^2** (3 equiv., 51 mg, 0.06 mmol) was dissolved in water (3 mL). The appropriate $LnCl_3{\cdot}xH_2O$ (1.1 equiv., 0.02 mmol) was added, and the reaction was kept at 70 °C for 3 h. The solvent was removed under reduced pressure, and ethanol was added. The suspension was heated under reflux for 1 h and then filtered through a P4 glass filter. The IR spectrum of the ligand shows a strong absorption in the IR region at $\tilde{\nu}$ = 1600 cm^{-1}, which corresponds to the C=O bond. After complexation, a new peak appeared at $\tilde{\nu} \approx$ 1500 cm^{-1}. The complexes have been characterized by TXRF, IR and optical spectroscopy. The Gd/Ln ratios obtained by TXRF spectroscopy were 3.0 (Gd/Tb), 3.0 (Gd/Dy), 3.0 (Gd/Eu), 2.9 (Gd/Sm), 2.7 (Gd/Nd) and 3.0 (Gd/Yb).

IR and NMR Spectroscopy: The FTIR spectra were recorded with a Bruker Vertex 70 FTIR spectrometer (Bruker, Ettlingen, Germany). The ^{1}H and ^{13}C NMR spectra were recorded by using a Bruker Avance 300 spectrometer (Bruker, Karlsruhe, Germany) operating at 300 MHz for ^{1}H and 75 MHz for ^{13}C or a Bruker Avance 400 spectrometer operating at 400 MHz for ^{1}H and 100 MHz for ^{13}C.

TXRF Spectroscopy: TXRF measurements were performed with a Bruker S2 Picofox instrument by analyzing approximately 100 ppm gadolinium solutions with respect to a Chem-Lab gallium standard solution (500 μg/mL, 2–5% HNO_3).

Optical Spectroscopy: The UV/Vis absorption spectra of freshly prepared aqueous solutions in quartz Suprasil® cells (115F-QS) with an optical pathlength of 0.2 cm were recorded with a Varian Cary 5000 spectrophotometer. The excitation data, emission data and luminescence decays were recorded with an Edinburgh Instruments FS920 steady-state spectrofluorimeter. This instrument was equipped with a 450 W xenon arc lamp, a high-energy microsecond flashlamp (μF900H) and an extended red-sensitive photomultiplier (185–1010 nm, Hamamatsu R 2658P). All spectra were corrected for the instrumental functions. The luminescence decays were determined under ligand excitation (293 and 315 nm), and the emission of the most intense transitions of the luminescent lanthanide ions was monitored. The luminescence decays were analyzed by using Edinburgh software, and the lifetimes were averages of at least three measurements in water and deuterated water. The quantum yields were determined by a comparative method with an estimated experimental error of 10% by using solutions of quinine sulfate (Fluka) in 1 N H_2SO_4 (Q = 54.6%) and rhodamine 101 (Sigma) in ethanol (Q = 100%) as standards. The solutions were diluted to provide an optical density of less than 0.05 at the excitation wavelength.

Proton NMRD: The proton NMRD profiles were measured with a Stelar Spinmaster FFC fast-field cycling NMR relaxometer [Stelar, Mede (PV), Italy] over a magnetic field strength range extending from 0.24 mT to 0.7 T. The measurements were performed at 310 K with samples (0.6 mL) in 10 mm o.d. Pyrex tubes. Additional relaxation rates at 20, 60, 300 and 500 MHz were obtained with Minispec mq-20, Minispec mq-60, Bruker Avance-300 and Bruker Avance 500 instruments (Bruker, Karlsruhe, Germany), respectively.

Acknowledgments

CHN microanalysis was performed by Mr Dirk Henot. The ESI-MS measurements were done by Mr Dirk Henot, and Mr Karel Duerinckx is acknowledged for his help with the NMR measurements. Mrs Corinne Piérart is acknowledged for her help in performing the relaxometric measurements.

[1] P. Hermann, J. Kotek, V. Kubícek, I. Lukes, *Dalton Trans.* **2008**, 3027–3047.
[2] V. C. Pierre, M. J. Allen, P. Caravan, *J. Biol. Inorg. Chem.* **2014**, *19*, 127–31.
[3] É. Tóth, L. Helm, A. Merbach, in: *Contrast Agents I* (Ed.: W. Krause), Springer, Berlin, **2002**, p. 61–101.
[4] P. Caravan, *Acc. Chem. Res.* **2009**, *42*, 851–62.
[5] E. Debroye, T. N. Parac-Vogt, *Chem. Soc. Rev.* **2014**, *43*, 8178–8192.
[6] W. P. Cacheris, S. C. Quay, S. M. Rocklage, *Magn. Reson. Imaging* **1990**, *8*, 467–481.
[7] F. G. Shellock, E. Kanal, *J. Magn. Reson. Imaging* **1999**, *10*, 477–484.
[8] A. Accardo, D. Tesauro, L. Aloj, C. Pedone, G. Morelli, *Coord. Chem. Rev.* **2009**, *253*, 2193–2213.
[9] P. Caravan, J. J. Ellison, T. J. McMurry, R. B. Lauffer, *Chem. Rev.* **1999**, *99*, 2293–2352.
[10] A. J. Villaraza, A. Bumb, M. W. Brechbiel, *Chem. Rev.* **2010**, *110*, 2921–2959.
[11] I. Solomon, *Phys. Rev.* **1955**, *99*, 559–565.
[12] P. Lebdušková, J. Kotek, P. Hermann, L. Vander Elst, R. N. Muller, I. Lukeš, J. A. Peters, *Bioconjugate Chem.* **2004**, *15*, 881–889.
[13] C.-H. Huang, K. Nwe, A. Al Zaki, M. W. Brechbiel, A. Tsourkas, *ACS Nano* **2012**, *6*, 9416–24.
[14] Y. Li, M. Beija, S. Laurent, L. vander Elst, R. N. Muller, H. T. T. Duong, A. B. Lowe, T. P. Davis, C. Boyer, *Macromolecules* **2012**, *45*, 4196–4204.
[15] G. Dehaen, S. V. Eliseeva, K. Kimpe, S. Laurent, L. Vander Elst, R. N. Muller, W. Dehaen, K. Binnemans, T. N. Parac-Vogt, *Chem. Eur. J.* **2012**, *18*, 293–302.

[16] M. Zhen, J. Zheng, L. Ye, S. Li, C. Jin, K. Li, D. Qiu, H. Han, C. Shu, Y. Yang, C. Wang, *ACS Appl. Mater. Interfaces* **2012**, *4*, 3724–3729.
[17] T. N. Parac-Vogt, K. Kimpe, S. Laurent, C. Piérart, L. V. Elst, R. N. Muller, K. Binnemans, *Eur. J. Inorg. Chem.* **2004**, 3538–3543.
[18] F. Kielar, L. Tei, E. Terreno, M. Botta, *J. Am. Chem. Soc.* **2010**, *132*, 7836–7837.
[19] E. Debroye, S. Laurent, L. Vander Elst, R. N. Muller, T. N. Parac-Vogt, *Eur. J. Inorg. Chem.* **2013**, 16019–28.
[20] S. Langereis, T. Geelen, H. Grüll, G. J. Strijkers, K. Nicolay, *NMR Biomed.* **2013**, *26*, 728–44.
[21] E. Debroye, S. V. Eliseeva, S. Laurent, L. Vander Elst, R. N. Muller, T. N. Parac-Vogt, *Dalton Trans.* **2014**, *43*, 3589–600.
[22] S. Aime, P. Caravan, *J. Magn. Reson. Im.* **2009**, *30*, 1259–67.
[23] R. T. M. de Rosales, *J. Labelled Compd. Radiopharm.* **2014**, *57*, 298–303.
[24] M. P. Placidi, J. Engelmann, L. S. Natrajan, N. K. Logothetis, G. Angelovski, *Chem. Commun.* **2011**, *47*, 11534–11536.
[25] G. Tallec, P. H. Fries, D. Imbert, M. Mazzanti, *Inorg. Chem.* **2011**, *50*, 7943–7945.
[26] B. P. Joshi, T. D. Wang, *Cancer* **2010**, *2*, 1251–87.
[27] G. Dehaen, P. Verwilst, S. V. Eliseeva, S. Laurent, L. Vander Elst, R. N. Muller, W. M. De Borggraeve, K. Binnemans, T. N. Parac-Vogt, *Inorg. Chem.* **2011**, *50*, 10005–10014.
[28] G. Dehaen, S. V. Eliseeva, P. Verwilst, S. Laurent, L. Vander Elst, R. N. Muller, W. De Borggraeve, K. Binnemans, T. N. Parac-Vogt, *Inorg. Chem.* **2012**, *51*, 8775–8783.
[29] E. Debroye, G. Dehaen, S. V. Eliseeva, S. Laurent, L. Vander Elst, R. N. Muller, K. Binnemans, T. N. Parac-Vogt, *Dalton Trans.* **2012**, *41*, 10549.
[30] E. Debroye, M. Ceulemans, L. Vander Elst, S. Laurent, R. N. Muller, T. N. Parac-Vogt, *Inorg. Chem.* **2014**, *53*, 1257–1259.
[31] C. Platas-Iglesias, C. Piguet, N. André, J.-C. G. Bünzli, *J. Chem. Soc., Dalton Trans.* **2001**, 3084–3091.
[32] T. Ohe, N. Miyaura, A. Suzuki, *J. Org. Chem.* **1993**, *58*, 2201–2208.
[33] A. Aebischer, F. Gumy, J.-C. G. Bünzli, *Phys. Chem. Chem. Phys.* **2009**, *11*, 1346–1353.
[34] H. Onishi, *Talanta* **1972**, *19*, 473–478.
[35] A. L. Gassner, C. Duhot, J.-C. G. Bünzli, A. S. Chauvin, *Inorg. Chem.* **2008**, *47*, 7802–7812.
[36] J.-C. G. Bünzli, S. V. Eliseeva, *Springer Ser. Fluoresc.* **2011**, 1–45.
[37] A. Beeby, I. M. Clarkson, R. S. Dickins, S. Faulkner, D. Parker, L. Royle, A. S. de Sousa, J. A. G. Williams, M. Woods, *J. Chem. Soc. Perkin Trans. 2* **1999**, 493–504.
[38] R. M. Supkowski, W. D. Horrocks, *Inorg. Chim. Acta* **2002**, *340*, 44–48.
[39] E. G. Moore, *Dalton Trans.* **2012**, *41*, 5272–5279.
[40] T. Kimura, Y. Kato, *J. Alloys Compd.* **1998**, *275–277*, 806–810.
[41] W. D. Horrocks, D. R. Sudnick, *J. Am. Chem. Soc.* **1979**, *101*, 334–340.
[42] M. Harris, S. Carron, L. Vander Elst, S. Laurent, R. N. Muller, T. N. Parac-Vogt, *Chem. Commun.* **2015**, *51*, 2984–2986.
[43] N. Bloembergen, *J. Chem. Phys.* **1957**, *27*, 572.
[44] J. Freed, *J. Chem. Phys.* **1978**, *68*, 4034–4037.
[45] M. Botta, *Eur. J. Inorg. Chem.* **2000**, 399–407.
[46] S. Laurent, L. Vander Elst, R. N. Muller, *Contrast Media Mol. Imaging* **2006**, *1*, 128–137.

Received: June 12, 2015
Published Online: August 7, 2015

